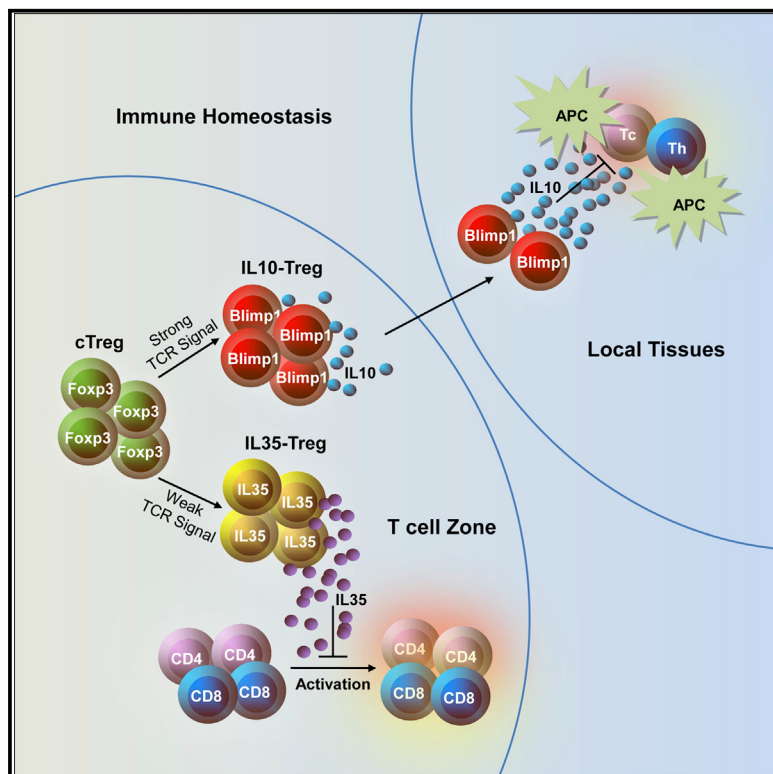


Reciprocal Expression of IL-35 and IL-10 Defines Two Distinct Effector Treg Subsets that Are Required for Maintenance of Immune Tolerance

Graphical Abstract



Authors

Xundong Wei, Jianhua Zhang,
Qianchong Gu, Man Huang, Wei Zhang,
Jie Guo, Xuyu Zhou

Correspondence

zhouxy@im.ac.cn

In Brief

Producing suppressive cytokines is a key molecular mechanism for Tregs to conduct long-range suppressive functions. Wei et al. demonstrated that effector Tregs can be diversified into two functionally distinct subsets based on IL-35 and IL-10 expression that work in a complementary way to maintain immune tolerance.

Highlights

- Expression of IL-35 and IL-10 defines two distinct subsets of Treg effectors
- IL-35-Tregs and IL-10-Tregs have different transcription factor dependency
- IL-35-Tregs and IL-10-Tregs have different activation status and geographic locations
- IL-35-Tregs and IL-10-Tregs cooperate to maintain immune tolerance

Data and Software Availability

GSE103456

Reciprocal Expression of IL-35 and IL-10 Defines Two Distinct Effector Treg Subsets that Are Required for Maintenance of Immune Tolerance

Xundong Wei,^{1,2} Jianhua Zhang,¹ Qianchong Gu,^{1,2} Man Huang,^{1,2} Wei Zhang,¹ Jie Guo,¹ and Xuyu Zhou^{1,2,3,4,*}

¹CAS Key Laboratory of Pathogenic Microbiology and Immunology, Institute of Microbiology, Chinese Academy of Sciences (CAS), Beijing 100101, China

²University of Chinese Academy of Sciences, Beijing 100049, China

³Savaid Medical School, University of Chinese Academy of Sciences, Beijing 101408, China

⁴Lead Contact

*Correspondence: zhouxy@im.ac.cn

<https://doi.org/10.1016/j.celrep.2017.10.090>

SUMMARY

Regulatory T cells (Tregs) can exert their functions through multiple suppressive mechanisms; however, it is unclear how Tregs exactly employ these mechanisms. In this study, we found that interleukin-35 (IL-35)-producing Tregs were a distinct effector population from the IL-10-producing subset. We also revealed that these two subsets of effector Tregs have different transcription factor dependency. Terminal differentiation regulator Blimp1 was only critical for IL-10 production, but not for IL-35; Foxp3 was essential for IL-35 but dispensable for IL-10 production. Furthermore, we demonstrated that IL-35-producing and IL-10-producing Tregs have a different activation status, do not share the same geographic locations in secondary lymphoid organs, and work in a complementary way to prevent autoimmunity. Thus, our study highlights the importance of effector Treg generation. We also provide evidence of Treg activation status tuning the generation of distinct effector Treg subsets, which work cooperatively to maintain immune tolerance.

INTRODUCTION

Regulatory T cells (Tregs) play a central role in maintaining immune self-tolerance and preventing autoimmune disease (Sakaguchi, 2004). Tregs are either generated in the thymus (tTregs) or peripherally (pTregs), and both specifically express the forkhead/winged-helix transcription factor Foxp3 (Abbas et al., 2013; Hori, 2014). Expression of Foxp3 is critical for Tregs to maintain their suppressive function and for self-tolerance of the immune system. Tregs can exert their functions through multiple suppressive mechanisms: (1) inhibitory cytokines release (interleukin-10 [IL-10], transforming growth factor β (TGF- β), and IL-35) (Bettini and Vignali, 2009; Pandiyan and Zhu, 2015); (2) granzyme-dependent cytolysis of target cells (Gondek et al., 2005); (3) metabolic disruption; and (4) modulation of antigen-presenting cell (APC) function (Vignali et al.,

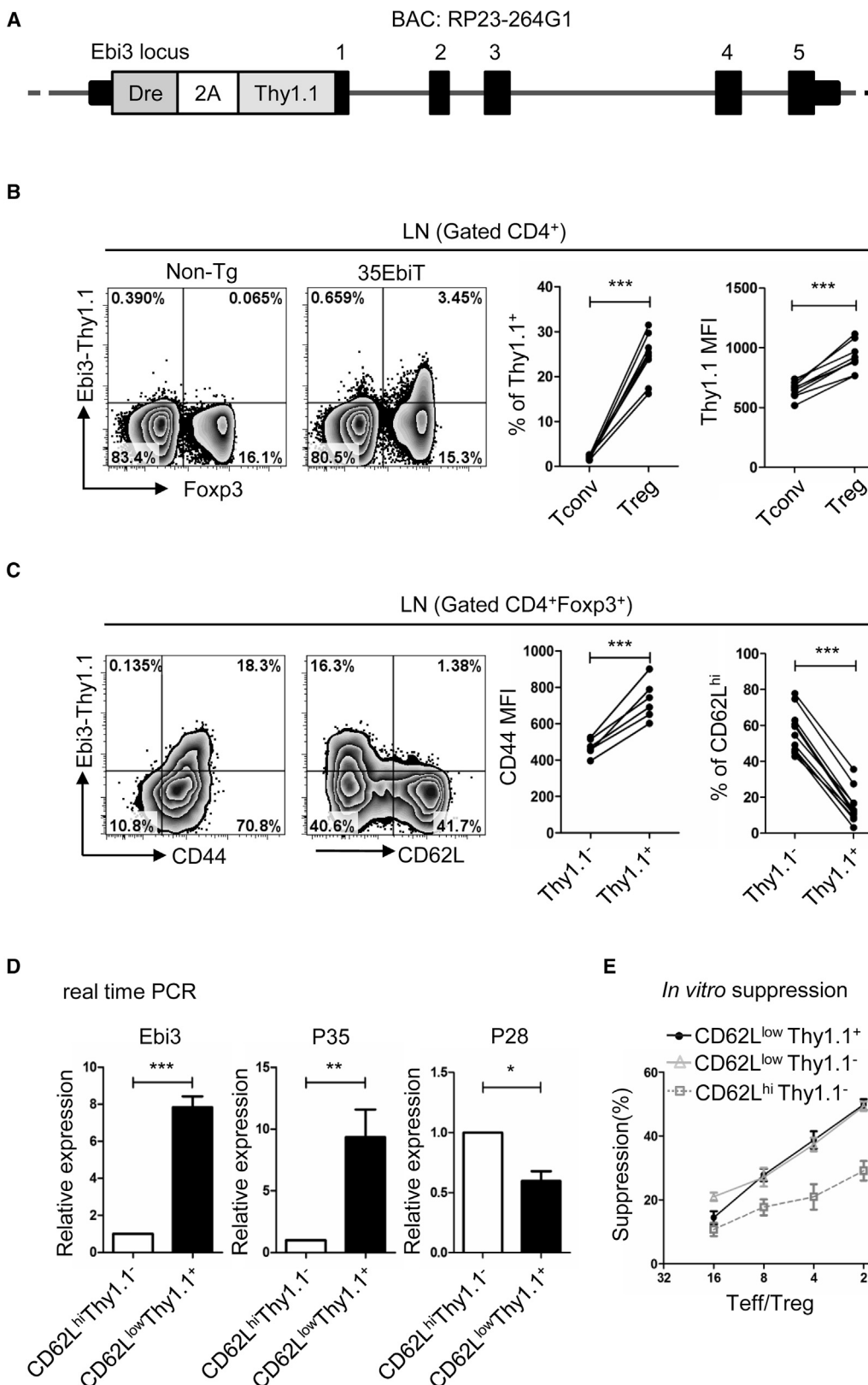
2008). However, it is unclear how Tregs exactly employ these mechanisms.

Tregs can be further specified as central Tregs (cTregs) or effector Tregs (eTregs) in peripheral lymphoid organs (Smigiel et al., 2014). cTregs (also defined as resting Tregs) occupy the major proportion of the Tregs in the secondary lymphoid organs and express high levels of CD62L and C-C chemokine receptor type 7 (CCR7), which are also highly expressed in naive T conventional cells (Tconv), contributing to their circulation between different lymphoid organs (Liston and Gray, 2014; Smigiel et al., 2014). In contrast, eTregs only account for a limited number of Tregs in the secondary lymphoid organs and express high levels of surface markers, such as CD44, inducible T cell costimulator (ICOS), and various chemokine receptors responsible for tissue location (Cretney et al., 2013; Smigiel et al., 2014). It is not clear whether eTregs are the major subset that directly conducts suppressive function *in vivo*. Emerging evidence indicates that T cell receptor (TCR) stimulation could be an important step for gaining appropriate suppressive function(s) by Tregs (Li and Rudensky, 2016). Recent studies showed that conditional deletion of TCR α after Treg maturation blocks eTreg generation and causes a severe autoimmune phenotype resembling scurfy mice; however, whether this phenotype is due to defective Treg activation and/or lacking TCR-derived survival signal still needs further investigation.

Production of inhibitory cytokines, such as IL-10, TGF- β , and IL-35, is a key feature of Tregs (Bettini and Vignali, 2009; Pandiyan and Zhu, 2015; Vignali et al., 2008). Moreover, TCR signaling is required for production of IL-10 and IL-35 (Levine et al., 2014). Transcription factors interferon regulatory factor 4 (IRF4) and Blimp1, two important downstream targets of TCR signaling (Cretney et al., 2011), are involved in many immunosuppressive functions of effector Tregs. Like many other cell types, in which IRF4 and Blimp1 play an important role in regulating terminal effector differentiation (Martins and Calame, 2008), their expression by effector Tregs is crucial for IL-10 production (Cretney et al., 2011). Aside from the well-documented inhibitory cytokines, such as IL-10, immunosuppressive cytokine IL-35 is associated with Treg cell function (Collison et al., 2007, 2010). IL-35, a member of the enigmatic IL-12 family and formed as a heterodimer composed of p35 (IL-12A) and Ebi3 (Epstein-Barr virus-induced gene 3), has strong suppressive properties both *in vivo* and *in vitro* (Bettini et al., 2012; Huang et al., 2011). It is



CrossMark



(legend on next page)

mainly secreted by Tregs, but not by Tconv cells, and specific knockout of Ebi3 or p35 in Tregs significantly compromises their suppressive activity (Collison et al., 2007). Recently, Turnis et al. further provided evidence of IL-35 in restricting anti-tumor immunity by using Treg-specific Ebi3 conditional knockout mice (Turnis et al., 2016). Unlike IL-10-producing Tregs, the characteristics of IL-35-producing Tregs, including their developmental origin, cellular phenotype, and specific function, are still unknown. This is largely due to the rapid secretion of IL-35 and the lack of a suitable antibody for intracellular IL-35 staining by flow cytometry.

In this study, we observed an unexpected expression pattern of IL-35 and IL-10 mRNA during Treg activation. To determine the characteristics and *in vivo* functions of IL-35-producing Tregs and further explore the differentiation of eTregs in detail, we generated an IL-35 reporter mouse (Ebi3-Dre-Thy1.1), which allowed us to distinguish Ebi3-expressing cells by using the surface expression of Thy1.1. Characterization of these mice demonstrated that effector Tregs can be diversified into two subsets based on their suppressive cytokine production: (1) IL-35-Tregs, which predominantly produce IL-35 and express intermediate levels of ICOS and CCR7, preferentially localize to the T cell zone of secondary lymphoid organs and play a role in damping the anti-tumor response; and (2) IL-10-Tregs, which produce high levels of IL-10, ICOS, and granzymes and express terminal differentiation regulator Blimp1 and a distinct set of chemokine receptors, such as CCR5 and CCR4, selectively migrate to peripheral tissues to repress local immune responses. Interestingly, Blimp1 was only crucial for IL-10 production but not for IL-35, whereas Foxp3 determined the expression of IL-35 in Tregs but not IL-10. Importantly, simultaneous ablation of the IL-35 and IL-10 Tregs resulted in a synergistic detrimental effect in maintaining tolerance. Together, our results provide convincing evidence that Tregs must be activated to conduct immune suppression; more importantly, we demonstrated a different Treg activation status could generate distinct Treg effector subsets, which play complementary roles in the maintenance of tolerance.

RESULTS

Distinct Expression Patterns of IL-35 and IL-10 mRNA during Treg Activation

Tregs undergo TCR stimulation, activation, and migration steps when they encounter antigens in the secondary lymphoid organs

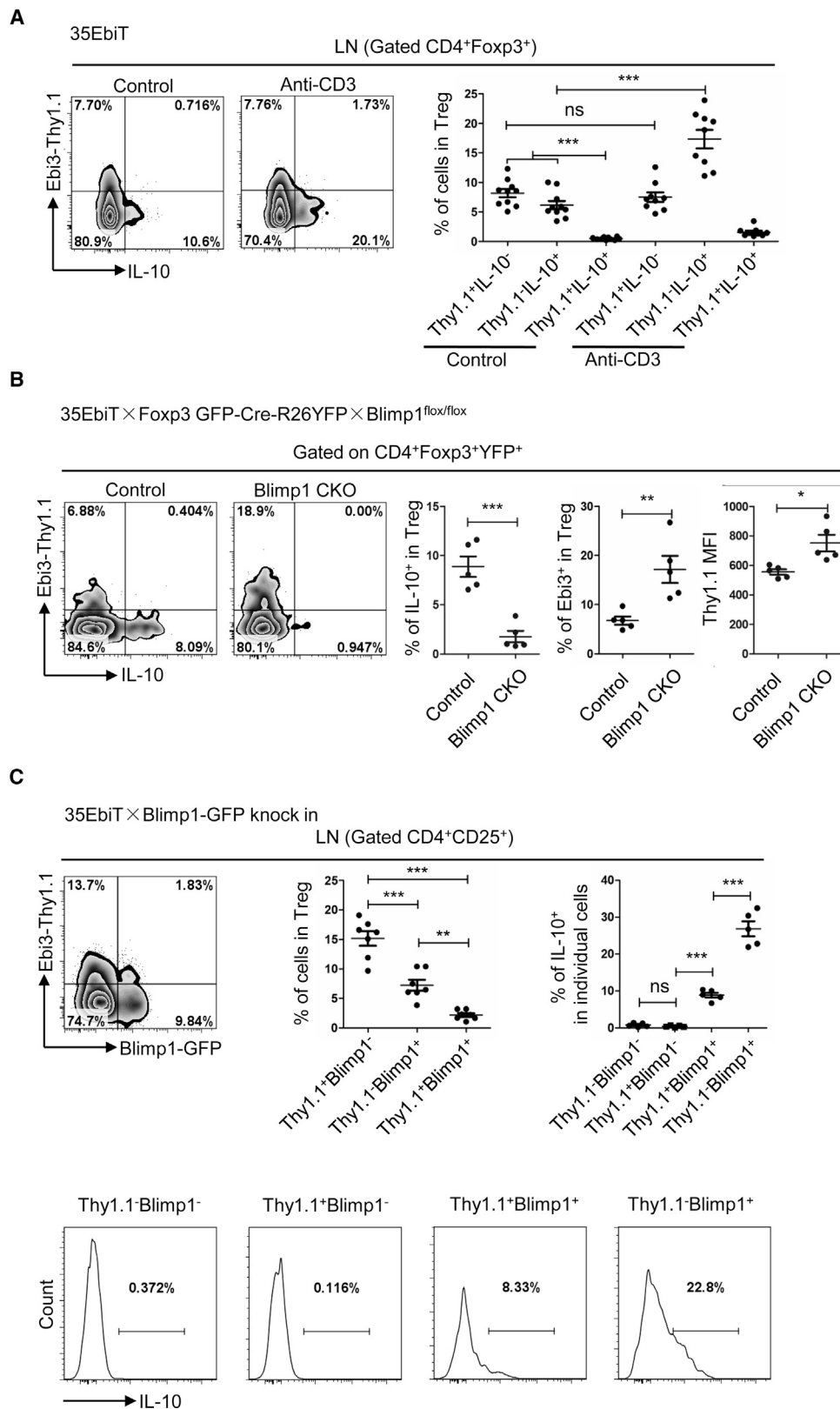
(Smigiel et al., 2014). To understand this activation procedure in detail, we combined two surface markers (CCR5 and ICOS) to determine Treg activation status. CCR5 is a chemokine receptor that is upregulated in all tissue-resident Tregs (Campbell, 2015; Ding et al., 2012; Moreira et al., 2008; Yurchenko et al., 2006), whereas ICOS, a potent costimulatory molecule, plays an important role in the maintenance of effector Treg survival. In addition, ICOS expression is controlled by TCR and CD28 signaling, gradually increasing following activation-induced proliferation (Smigiel et al., 2014). Interestingly, we observed that CCR5 expression by Tregs in the lymph node is restricted to the ICOS^{high} population (Figure S1A). To gain functional insights into the different subsets of effector Tregs, we purified CD62L^{lo}ICOS^{med}CCR5⁻ and CD62L^{lo}ICOS^{hi}CCR5⁺ Tregs and compared them to the resting (CD62L^{high}ICOS⁻CCR5⁻) subset for gene expression that is related to Treg suppressive activity by using real-time PCR (Figure S1B). Notably, we found that Ebi3, a subunit of IL-35, displays a unique expression pattern. Unlike IL-10 and its key transcription regulator Blimp1 (Cretney et al., 2011), which were induced in CD62L^{lo}ICOS^{hi}CCR5⁺, induction of Ebi3 was predominately detected in the CD62L^{lo}ICOS^{med}CCR5⁻ subset. Thus, two major suppressive cytokines, IL-10 and IL-35, are secreted by different populations of eTreg.

Generation of the Ebi3 Reporter Mice

Although both Tregs and *in vitro* generated CD4⁺Foxp3⁻ “iT35” T cells are reported to produce the immunosuppressive cytokine IL-35 (Collison et al., 2010). The detailed phenotypes and specific function of IL-35-producing cells are still poorly characterized under *in vivo* physiological conditions. To trace IL-35-expressing cells, we generated IL-35 reporter mice that carry genes encoding Dre recombinase and the Thy1.1 surfaced protein linked by a “self-cleaving” 2A peptide under the control of a BAC Ebi3 promoter (Figure 1A) (Szymczak et al., 2004). The transgenic mouse lines, herein referred to as 35EbiT mice, generated by pronucleus microinjection of a modified BAC, developed normally and had no immunological abnormalities across their lifespan. Thy1.1 expression was not found in NK, NKT, CD8, peritoneal macrophages, dendritic cells (DCs), and B cells, but was clearly detectable in a subset of CD4 T cells in 35EbiT mice (Figure S2A). Co-staining of Foxp3 with Thy1.1 showed that the large majority of Thy1.1⁺ T cells was also positive for Foxp3 expression, and the mean fluorescence

Figure 1. Generation and Characterization of the Transgenic Ebi3 Tracer Mice

- (A) The BAC transgenic construct used to generate Ebi3 reporter mice. A reporter cassette consisting of the coding sequence of the *Dre* and *Thy1.1* genes was introduced downstream of the *Ebi3* translational start site.
 - (B) Flow cytometry of lymph node CD4⁺ T cells isolated from 35EbiT transgenic mice or wild-type littermates. Cells were stained for CD4, Thy1.1, and intracellular Foxp3. Numbers in the plots indicate the percentage of cells in each quadrant (left). The average frequency of Thy1.1⁺ cells and the MFI of Thy1.1 are shown (right). See also Figures S2A–S2C.
 - (C) CD44, CD62L, and Thy1.1 (Ebi3) expression levels on CD4⁺Foxp3⁺ cells from the lymph nodes of 35EbiT transgenic mice. See also Figure S2D.
 - (D) qRT-PCR analysis of *Ebi3*, *P35*, and *P28* mRNA expression in sorted Thy1.1⁺ (CD4⁺GFP⁺CD62L^{low}Thy1.1⁺) and Thy1.1⁻ (CD4⁺GFP⁺CD62L^{hi}Thy1.1⁻) Tregs from the lymph nodes of 35EbiT × Foxp3-GFP KI dual reporter mice. Thy1.1⁺ cells from 35EbiT transgenic mice faithfully report IL-35 expression. Results are presented relative to the expression of GAPDH.
 - (E) Proliferation of responder T cells cultured *in vitro* at various ratios (horizontal axis) with CD4⁺YFP⁺CD62L^{low}Thy1.1⁺, CD4⁺YFP⁺CD62L^{low}Thy1.1⁻, and CD4⁺YFP⁺CD62L^{hi}Thy1.1⁻ sorted from the lymph nodes of 35EbiT × Foxp3GFP-Cre-R26YFP triple transgenic mice.
- The data shown are typical results from >3 experiments. Each symbol represents an individual mouse, n ≥ 5; small horizontal bars indicate mean ± SEM; ns, not significant; *p < 0.05; **p < 0.01; and ***p < 0.001 (Student's t test). See also Figure S3.



(legend on next page)

intensity (MFI) of Thy1.1 in $\text{Foxp3}^+\text{Thy1.1}^+$ cells was significantly higher than in $\text{Foxp3}^-\text{Thy1.1}^+$ cells (Figure 1B), which is consistent with previous results showing that IL-35 is an immunosuppressive cytokine mainly produced by Tregs (Collison et al., 2007). The percentage of Thy1.1^+ cells increased with age (Figure S2B), and their abundance was variable in the lymphoid organs (Figure S2C). Notably, Tregs from peripheral blood contained a much lower percentage of Thy1.1^+ cells than the lymph node (LN), spleen, and all other organs (Figure S2C). A previous study demonstrated that self-antigen engagement can trigger partial TCR signaling manifested by CD3 zeta phosphorylation, which mainly occurs in the secondary lymphoid organs but not in peripheral blood (Stefanová et al., 2002). Thus, we checked for the T cell activation markers CD44 and CD62L in the Foxp3^+ subset. As shown in Figure 1C, Thy1.1^+ populations were activated Treg cells, exclusively CD62L^{lo} , and express much higher levels of CD44. Moreover, Thy1.1^+ Tregs expressed higher levels of ICOS, CD38, CD69, CD103, CTLA-4, PD1, and GITR, lower levels of Bcl2, and a similar amount of CD25 compared to Thy1.1^- Tregs, further confirming their effector Treg phenotypes (Figure S2D). Thy1.1^+ Tregs also displayed a much higher percentage of Helios and Neuropilin-1 (Figure S2D), indicating their thymic origin. To further ensure the accuracy of reporter expression in the 35EbiT mice, we measured the mRNA expression of endogenous *Ebi3*, *p35*, and *p28* in $\text{CD4}^+\text{Foxp3}^+\text{CD62L}^{\text{low}}\text{Thy1.1}^+$ and $\text{CD4}^+\text{Foxp3}^+\text{CD62L}^{\text{hi}}\text{Thy1.1}^-$ T cells, respectively (Figure 1D). As expected, Thy1.1^+ populations expressed significantly higher levels of both endogenous *Ebi3* and *p35* mRNA but not *p28* mRNA compared to Thy1.1^- populations. In correlation to their activation phenotype, we found that Thy1.1^+ Treg cells were more potent suppressors of the proliferation of Tconv cells *in vitro* than that of central Treg cells (Figure 1E). Together, these results indicated that the surface Thy1.1 expression in 35EbiT transgenic mice serves as a reliable marker for endogenous IL-35 expression.

IL-35 Induction Is Controlled by Foxp3 Expression

Next, we ask whether resting-like central Tregs could induce IL-35 expression upon lymph proliferation. We obtained $\text{CD4}^+\text{CD62L}^{\text{hi}}\text{GFP}^+\text{Thy1.1}^-$ from 35EbiT × Foxp3-GFP KI reporter mice and intravenously transferred them into $\text{TCR}\beta^{-/-}$ recipients for 15 days. As shown in Figure S3A, 20%–40% of central Tregs induced IL-35 expression after transfer. Interest-

ingly, we noticed a substantial percentage of the Tregs lost Foxp3 expression after 15 days post-transfer, and, more importantly, a much lower level of Ebi3 expression was observed in those exFoxp3 cells (Figure S3A). This result suggested that IL-35 production by Tregs is likely determined by their master regulator Foxp3, which corresponds with previous studies demonstrating that overexpression of Foxp3 in Tconv CD4⁺ T cells promotes IL-35 mRNA production (Collison et al., 2007). To exclude any artificial possibility from the adoptive transfer mode, we utilized the Foxp3 fate-mapping system (35EbiT × Foxp3GFP-Cre × R26YFP) by examining Thy1.1 expression in various Treg populations with different Foxp3 expression levels (Zhou et al., 2009). Based on the expression level of Foxp3, yellow fluorescent protein (YFP)-traced Tregs were divided into three subsets in the fate-mapping mice: Foxp3^{hi}, Foxp3^{low}, and Foxp3^{neg} (exFoxp3) (Figure S3B). As shown in Figure S3B, Foxp3^{hi} populations possessed the highest percentage of *Ebi3*⁺ Treg cells in the lymph node, spleen, and Peyer's patches, whereas the numbers of *Ebi3*⁺ Treg cells decline gradually in Foxp3^{low} and negative populations (Figure S3B). Thus, IL-35 induction was strongly associated with Foxp3 levels in the CD4 T cells.

Recent studies suggest that Foxp3 needs to couple with Treg-specific epigenetic reprogramming (Treg-Me) to establish the real Treg lineage (Ohkura et al., 2012). Thus, the lack of IL-35 expression by exFoxp3 cells could be due to either failure to gain Treg-specific epigenetic reprogramming during the early development stage or later loss of Foxp3 expression. To test this possibility, we crossed 35EbiT with Foxp3 knockout and Foxp3GFP-Cre-R26YFP mice to generate a 35EbiT × Foxp3GFP-Cre-R26YFP-Foxp3 knockout heterozygote strain. In the female mice from this strain, half of the YFP⁺ cells express wild-type Foxp3 and the other half express mutant Foxp3 ("wannabe" Treg) due to X chromatin inactivation. A previous study documents that the establishment of Treg-specific epigenetic reprogramming does not rely on Foxp3 expression, and these wannabe Tregs have a similar Treg cell-type CpG hypomethylation pattern as wild-type Tregs (Ohkura et al., 2012). As shown in Figure S3C, Treg-specific epigenetic reprogramming was not enough to induce IL-35, and expression of IL-35 was severely impaired in the wannabe Tregs. Together, these results demonstrated that Foxp3 itself, rather than Treg-specific epigenetic reprogramming, determines IL-35 induction by Tregs.

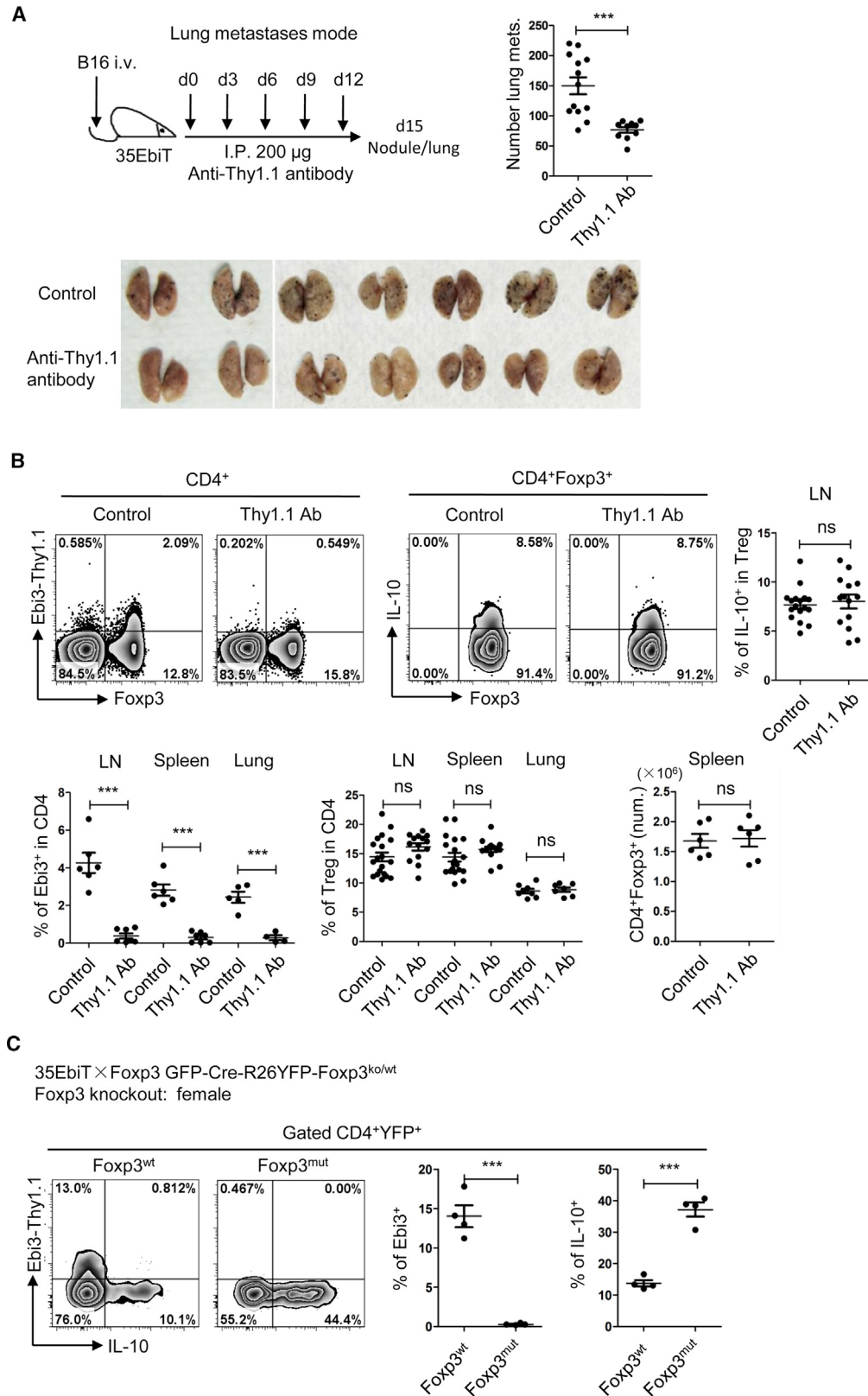
Figure 2. Expression of Ebi3 and IL-10 Defines Two Distinct Populations of Treg Effectors

(A) 35EbiT mice were treated with PBS (control) or anti-CD3 (2 µg/time intravenous [i.v.]) five times with an interval of 2 days, and sacrificed 12 hr after the final injection. Plots represent the expression of IL-10 and Thy1.1 (Ebi3) by lymph node CD4⁺Foxp3⁺ cells after PBS or anti-CD3 antibody treatment (left). Average frequencies of *Ebi3*⁺IL-10⁻, *Ebi3*⁻IL-10⁺, and *Ebi3*⁺IL-10⁺ cells among CD4⁺Foxp3⁺ cells from antibody-treated mice relative to PBS-treated mice are shown (right). See also Figure S1.

(B) Flow cytometry of lymphocyte samples from control mice (35EbiT × Foxp3GFP-Cre-R26YFP) and Blimp1 CKO mice (35EbiT × Foxp3GFP-Cre-R26YFP × Blimp1^{foxi/foxi}). Plots were gated on CD4⁺Foxp3⁺YFP⁺ Treg cells and analyzed for the expression of the Thy1.1 (Ebi3) reporter and intracellular IL-10 (left). Average frequencies of IL-10⁺ and Thy1.1⁺ (Ebi3) cells and the MFI of Thy1.1 among wild-type Tregs or Blimp1 knockout Tregs are shown (right). See also Figure S4.

(C) Flow cytometry of lymph node lymphocyte samples from 35EbiT × Blimp1-GFP KI reporter mice. Plots represent the expression of GFP (Blimp1) and Thy1.1 (Ebi3) by lymph node CD4⁺CD25⁺ cells (upper left). Average frequencies of Thy1.1⁺Blimp1⁻, Thy1.1⁻Blimp1⁺, and Thy1.1⁺Blimp1⁺ cells among CD4⁺CD25⁺ cells are shown (upper middle). Flow cytometry analysis for expression of IL-10 by each cell subset is shown (below). The average frequency of IL-10⁺ cells among gated subsets is shown (upper right).

The data shown are typical results from three experiments, n ≥ 9 (A); n = 5 (B); and n ≥ 5 (C). Each symbol represents an individual mouse; small horizontal bars indicate mean ± SEM; ns, not significant; *p < 0.05; **p < 0.01; and ***p < 0.001 (ANOVA with Bonferroni post-test [A and C] or Student's t test [B]).



(legend on next page)

Expression of Ebi3 and IL-10 Defines Two Distinct Subsets of Treg Effectors

After validating the fidelity of our 35EbiT mice, we performed intracellular IL-10 cytokine staining to measure IL-10 and IL-35 expression by Tregs using flow cytometry. Strikingly, we found that IL-35 and IL-10 are secreted by two distinct populations, with a very limited number of Thy1.1⁺IL-10⁺ (<1%) double-positive cells being found in Tregs from the secondary lymphoid organs (Figure 2A). It has been reported that consecutive injection of anti-CD3 antibody boosts the production of IL-10 by Tregs (Kamanaka et al., 2006), and thus we adopted this approach to determine if CD3 antibody treatment also increases the number of Ebi3⁺ Treg cells in the 35EbiT mice. Indeed, the percentage of IL-10 increased significantly after administration of the CD3 antibody, but neither Ebi3⁺ Treg cells nor the rare population of Ebi3⁺IL10⁺ double-positive Tregs were affected by anti-CD3 stimulation (Figure 2A). These results are consistent with earlier real-time PCR data, demonstrating that the two major suppressive cytokines IL-35 and IL-10 are reciprocally expressed by distinct populations of Tregs.

Blimp1 is a transcriptional repressor expressed in most effector Tregs and plays a critical role in IL-10 production (Cretney et al., 2011). To assess the potential contribution of Blimp1 to IL-35 regulation, we crossed 35EbiT × Foxp3GFP-Cre-R26YFP mice with Blimp1^{flox/flox} mice to obtain Treg-specific conditional Blimp1 knockout mice (referred as Blimp1 CKO). As shown in Figure 2B, Blimp1-deficient Treg cells were incapable of producing IL-10 following phorbol 12-myristate 13-acetate (PMA) and ionomycin stimulation, whereas in sharp contrast, there was a 2-fold increase in the percentage of Ebi3⁺ Tregs in Blimp1-deficient Treg cells (Figure 2B). Clearly, Blimp1 was not an essential transcription factor for inducing IL-35 production by Tregs. To further understand the relationship between Blimp1 and IL-35, we crossed 35EbiT mice with Blimp1-GFP knockin reporter mice to generate a dual reporter mouse model and analyzed Ebi3 expression in Blimp1-positive and -negative populations (Figure 2C). Similarly, most IL-35 producing Thy1.1⁺ Treg cells and Blimp1⁺ Treg cells also fell into two distinct subpopulations; Ebi3⁺Blimp1⁺ double Treg cells were detectable but at a significantly lower frequency (Figure 2C). We further assessed IL-10 production by using this dual reporter mouse. In agreement with a previous study, <1% of Thy1.1⁻Blimp1⁻ cells produced

IL-10, and 20%–30% of Thy1.1⁻Blimp1⁺ single-positive Tregs produced IL-10, respectively. In contrast, the Thy1.1⁺Blimp1⁻ subset produced almost no IL-10, and the Thy1.1⁺Blimp1⁺ double-positive Treg subset produced IL-10 but much less than that of the Thy1.1⁻Blimp1⁺ Treg cells (Figure 2C). The large majority of Ebi3⁺ is not expressing Blimp1, which raises a question of why Blimp1 CKO mice have a much higher percentage of Ebi3⁺ Tregs. A simple interpretation could be Blimp1 directly suppresses Ebi3 transcription, thus relieving the inhibition by knockout of Blimp1, which would allow generation of more Ebi3⁺ Tregs. However, a higher percentage of Ebi3⁺ Tregs could also be an indirect effect caused by the autoimmune disorder observed in Blimp1 knockout mice. To test these possibilities, we have generated a healthy Treg-specific Blimp1 knockout mouse by using a Foxp3^{YFP-Cre} knockin strain. In the heterozygote female Foxp3^{YFP-Cre/wt} Blimp1 CKO mice, half of the wild-type Tregs could efficiently maintain the immune tolerance. As shown in Figure S4, the percentage of Ebi3 from Blimp CKO was comparable with the control mice. Therefore, Blimp1 is unlikely a direct inhibitor of IL-35 expression. Together, although Blimp1 is considered a key transcriptional regulator for effector Tregs, our results revealed that Ebi3-producing Tregs are predominantly Blimp1 independent.

To further investigate the reciprocal relationship between IL-35- and IL-10-producing Tregs, we took advantage of the surface expression of Thy1.1 in the 35EbiT reporter mice and performed *in vivo* depletion experiments with a Thy1.1-specific monoclonal antibody. Previous studies show that Treg secretion of IL-35 is involved in preventing anti-tumor immunity (Turnis et al., 2016). Thus, targeting Ebi3⁺ cells via antibody-mediated depletion could potentially boost the anti-tumor immune response. Therefore, we established a mouse metastatic tumor model by intravenously administering the B16 melanoma cell line and performed the injection of the Thy1.1 antibody to ablate Ebi3⁺ cells (Komatsu and Hori, 2007). At the end point, mice that received Thy1.1 antibody or control treatment were euthanized to determine the number of lung metastases (Figures 3A and S5). Consistently, the number of metastases was significantly reduced in the lungs of mice receiving Thy1.1 antibody after B16 transfer. Moreover, Ebi3⁺ cells in 35EbiT mice were substantially reduced after the injection of Thy1.1 antibody, whereas the total percentage of Treg cells in the CD4⁺ T cell population

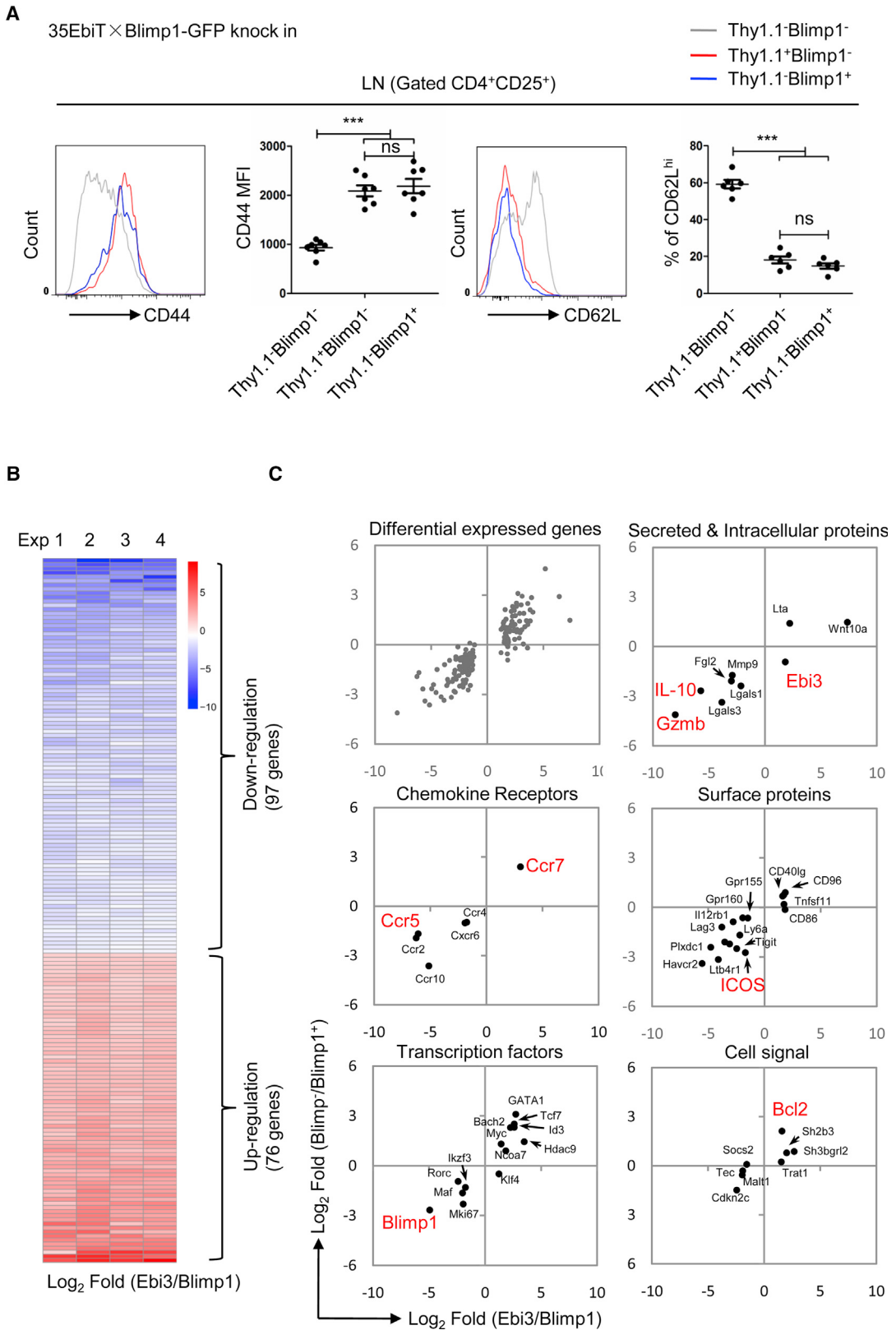
Figure 3. Ebi3⁺ Tregs Plays a Unique Role in Damping the Anti-Tumor Response

(A) 35EbiT transgenic mice were injected on day 0 with tumor cells (4×10^5 B16 i.v.) and received administration of anti-Thy1.1 antibody (200 µg/time i.p.). Antibody was injected five times with an interval of 2 days, and the mice were sacrificed 2 days after the final injection. The control mice were injected with PBS (upper left). Photographs of lungs from control or anti-Thy1.1 antibody-treated mice are shown (below); lung metastases were counted by microscopy (upper right). See also Figure S5.

(B) Frequency of Thy1.1⁺ (Ebi3) cells and Foxp3⁺ (Treg) cells among the CD4⁺ cells of the indicated organs from control or anti-Thy1.1 antibody-treated mice (upper left and below). The absolute cell numbers of the Tregs are shown on the bottom right. Graph representing the expression of IL-10 by lymph node CD4⁺Foxp3⁺ cells after PBS or anti-Thy1.1 antibody treatment (upper right). Cells were isolated and immediately stained with surface marker (Isotype Rat immunoglobulin G [IgG] and Thy1.1 Ab (19E12, Isotype Mouse IgG2a) at 4°C for 30 min, then stained with phycoerythrin (PE)-conjugated anti-Mouse IgG2a (m2a-15F8, Isotype Rat IgG1) and Foxp3.

(C) Foxp3 knockout heterozygote mice were crossed with Foxp3GFP-Cre and R26YFP (35EbiT × Foxp3GFP-Cre-R26YFP) male mice to generate a 35EbiT × Foxp3 GFP-Cre-R26YFP-Foxp3^{ko/wt} heterozygote strain. Plots represent the expression of Thy1.1 (Ebi3) and IL-10 by YFP⁺Foxp3^{wt} or YFP⁺Foxp3^{mut} cells from 35EbiT × Foxp3GFP-Cre-R26YFP-Foxp3^{ko/wt} female mice. The average frequency of Thy1.1⁺ (Ebi3) and IL-10⁺ cells among the Foxp3^{wt} or Foxp3^{mut} subset are shown.

The data shown are typical results from 3 experiments; n ≥ 6 (A and B); n = 4 (C). Each symbol represents an individual mouse; small horizontal bars indicate mean ± SEM; ns, not significant; **p < 0.001 (Student's t test).



(legend on next page)

was largely intact in the treated mice (**Figure 3B**). Importantly, depletion of Ebi3⁺ cells did not affect IL-10 secretion by CD4⁺Foxp3⁺ Treg cells (**Figure 3B**). Furthermore, we genetically removed Foxp3 by using the 35EbiT × Foxp3GFP-Cre-R26YFP × Foxp3 knockout heterozygote female strain, in which the expression of IL-35 was severely impaired in the Foxp3 mutant cells (**Figures 3C** and **S3C**); surprisingly, we found IL-10 production was not diminished and even increased about 3-fold in those Foxp3 mutant cells (**Figure 3C**). Thus, Foxp3 expression was only crucial for the generation of IL-35-producing Tregs but not for IL-10. Together, these results demonstrated that Ebi3⁺ Tregs and IL-10-producing Tregs are two distinct effector Treg subsets with different transcriptional factor dependency.

Profiling of Ebi3-Tregs and Blimp1-Tregs

To gain in-depth information about the two subsets of effector Tregs, we next performed RNA-seq analysis to compare the transcriptomes of Thy1.1⁺Blimp1⁻ (Ebi3-Tregs) and Thy1.1⁻Blimp1⁺ (Blimp1-Tregs) Tregs. Although the expression of CD44 and CD62L by Ebi3-Tregs and Blimp1-Tregs was identical (**Figure 4A**), Ebi3-Tregs possessed a distinct transcriptional profile compared to Blimp1-Tregs. We found ~173 unique genes with differential expression between the two effector subsets (**Figure 4B; Table S1**), in which Blimp1 and IL-10 were highly expressed in Blimp1-Tregs, whereas Ebi3 was enriched in the Ebi3-Tregs, respectively. Of note, the large majority of differentially expressed genes were also found in the pool of genes that were differentially expressed in Blimp1⁻ versus Blimp1⁺ Tregs (**Vasanthakumar et al., 2015**), suggesting that Blimp1 expression may largely contribute to the distinction between the Ebi3-Treg and Blimp1-Treg subsets (**Figure 4C**).

In agreement with the earlier qPCR results from the wild-type mice (**Figure S1B**), markers correlating with TCR activation and regulation, such as ICOS, TIGIT, Lag3, HAVCR2 (Tim3), Ltb4r1, and Ly6a, were highly expressed by Blimp1-Tregs, confirming the differential activation statuses of Ebi3-Tregs and Blimp1-Tregs. In addition, multiple genes that are related to cell migration to tissue (e.g., CCR5, CCR4, CCR10, CCR2, and CXCR6) were highly expressed by Blimp1-Tregs. In contrast, CCR7, the major chemokine receptor that guides Treg localization into the T-zone in secondary lymphoid organs, was enriched in Ebi3-Tregs (**Figure 4C**). We verified the differential expression of various genes by flow cytometry. CCR5, CCR4, ICOS, Ly6a, and TIGIT were expressed at the highest levels on Blimp1-Tregs,

the lowest in Thy1.1⁻Blimp1⁻ Tregs, and at an intermediate level in Ebi3-Tregs. Although they were not identified as differentially expressed by RNA-seq, other activation-related genes, such as CTLA-4 and CD39, also fell into this category, whereas a reverse pattern was found for CCR7 and Bcl2 expression (**Figure 5A**). To measure the TCR signal strength in Ebi3-Tregs and Blimp1-Tregs, we also compared the expression of CD5, which is a surface marker and correlates with the TCR signal strength. Indeed, Blimp1-Tregs have a higher CD5 surface expression (**Figure 5A**). More interestingly, we noticed that transcripts encoding proteins related to Treg-suppressive function, such as GzmB, Fgl2, Mmp9, Lgals1, and Lagl3, were preferentially enriched in the Blimp1-Treg subset (**Mari et al., 2016; Shalev et al., 2008; Vignali et al., 2008**). High levels of GzmB expression in Blimp1-Tregs were further confirmed by using real-time PCR (**Figure 5B**), implying that the two types of effectors may utilize distinct suppressive mechanisms other than through production of different cytokines. Ebi3-Tregs and Blimp1-Tregs also differentially expressed various transcription factors: Maf and Iκzf3 were enriched in Blimp1-Tregs, whereas Ebi3-Tregs expressed higher levels of Bach2, Tcf7, Id3, and GATA1, which were also enriched in resting cTregs (**Figure 4C**).

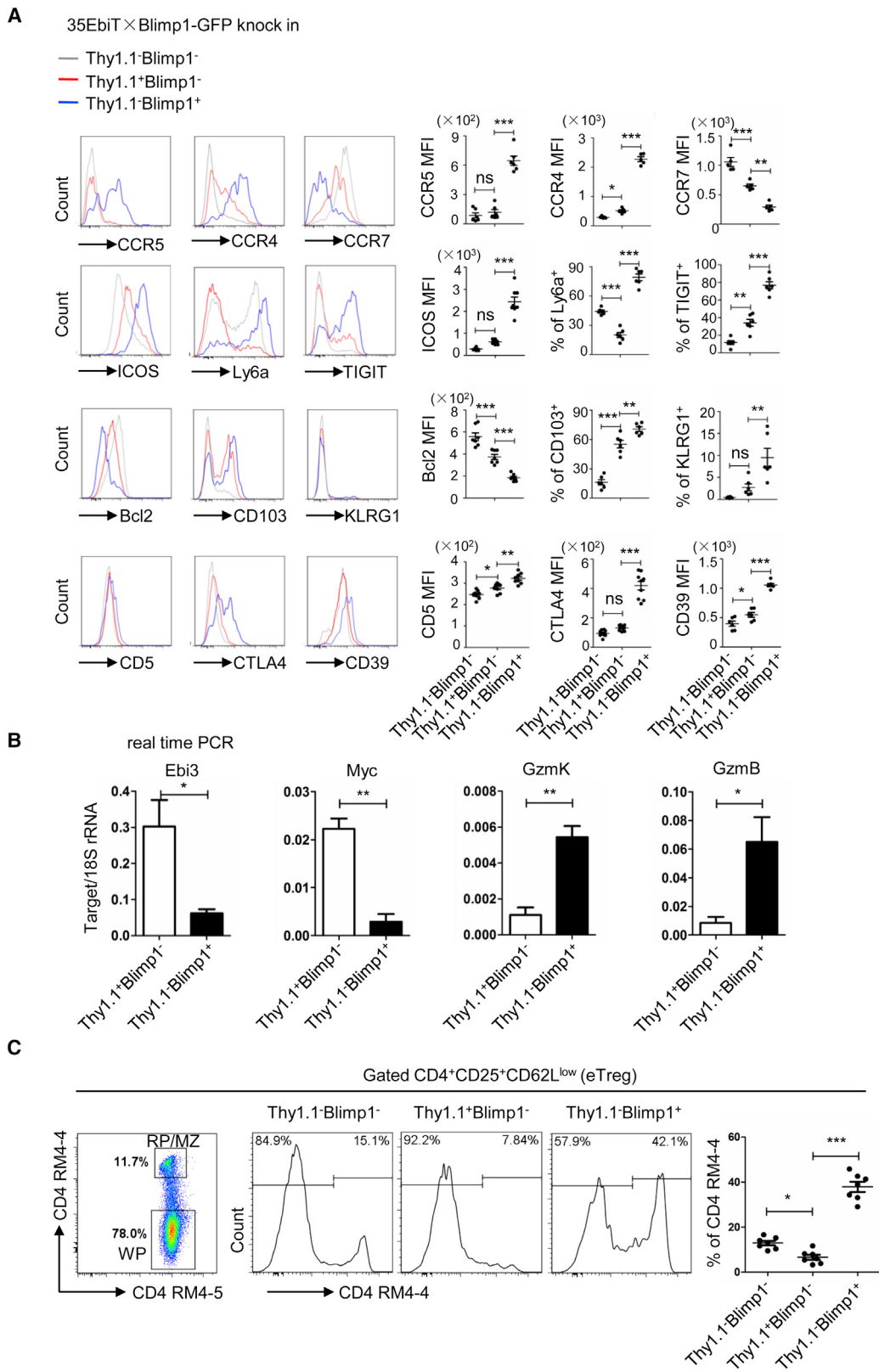
Expression of different chemokine receptors indicates distinct geography. Ebi3-Tregs may exert their suppressive functions in the T cell zone, and Blimp1-Tregs may more easily migrate to local inflammation sites. To test this possibility, we injected 35EbiT × Blimp1-GFP KI mice with the CD4 antibody (RM4-4) for 5 min *in vivo* and labeled the migrating T cells distributing at the red pulp and marginal zone (MZ) of the spleen. In agreement with previous studies showing that Blimp1-Tregs have a preference to locate outside of the T cell zone (**Vasanthakumar et al., 2015**), approximately 40% of Blimp1-Tregs stained positive by *in vivo* CD4 (RM4-4) antibody injection. In contrast, many fewer (<10%) Ebi3-Tregs were labeled (**Figure 5C**). Collectively, these results further support the notion that the two different Treg effectors have distinct activation statuses, do not share the same geographic locations, and might conduct a different suppressive function through distinct mechanisms.

Genetic Tracing of Ebi3-Tregs

Different activation status in IL-35- and IL-10-producing Tregs also raises a question that whether two effector subsets are representative of two stages of eTreg differentiation or two distinct populations. To clarify the developmental relationship between IL-35- and IL-10-Tregs, we performed genetic fate

Figure 4. Transcriptional Profiling of Ebi3-Treg and Blimp1-Treg Cells

- (A) Flow cytometry analysis of the lymph node CD4⁺CD25⁺ T cells from 35EbiT × Blimp1-GFP KI reporter mice. Histogram plots represent the expression of CD44 and CD62L by Thy1.1⁻Blimp1⁻ (gray line), Thy1.1⁺Blimp1⁻ (red line), and Thy1.1⁻Blimp1⁺ (blue line) cells. The percentages and MFI of the indicated markers are shown.
 - (B) Ebi3-Treg (CD4⁺CD25⁺Thy1.1⁺Blimp1⁻) and Blimp1-Treg (CD4⁺CD25⁺Thy1.1⁻Blimp1⁺) fractions from 35EbiT × Blimp1-GFP KI reporter mice were purified by FACS and then used for RNA-seq analysis. Heatmap of selected genes (log₂ fold change) that are differentially expressed (>2-fold) between Ebi3-Tregs and Blimp1-Tregs is shown for quadruplicate samples. Colors indicate upregulated (red) and downregulated (blue) genes in the Ebi3-Treg subset compared to the Blimp1-Treg subset (quadruplicate samples are shown). See also **Table S1**.
 - (C) Genes or selected genes differentially expressed in Ebi3-Treg (CD4⁺CD25⁺Thy1.1⁺Blimp1⁻) versus Blimp1-Treg (CD4⁺CD25⁺Thy1.1⁻Blimp1⁺) cells plotted against those expressed differently in Blimp1⁻ (CD25⁺Blimp1⁻) versus Blimp1⁺ (CD25⁺Blimp1⁺) Treg cells (**Vasanthakumar et al., 2015**).
- The data shown are the typical results of >3 experiments (A), n = 7. Data are representative of two experiments with four replicates, with three or more mice per replicate (B and C). Each symbol represents one individual mouse. Error bars represent mean ± SEM; ns, not significant; ***p < 0.001 (ANOVA with Bonferroni post-test).



(legend on next page)

mapping by crossed the 35EbiT mice with the Rosa26-rox-tdTomato tracer strain. In resultant mice, Dre expression in Ebi3⁺ cells allow excision of the Rox-flanked Rluc-stop cassette and drives constitutive transcription of tdTomato, permanently labeling the Ebi3⁺ cells and their progeny (Figure S6A). Unexpectedly, tdTomato expression was detectable in many different cell types, including a small subset of Lin⁻ Scal-1⁺c-Kit⁺ hematopoietic stem cells (Figures S6B and S6C), indicating that Ebi3 gene could be turned on in a certain period time, even before lymphocyte development. To exclude the influence of tdTomato expression from early development, we adoptively transferred peripheral mature CD4⁺tdTomato⁻ cells that sorted from pooled lymph nodes and the spleen of Ebi3 lineage tracer mice intravenously into TCR $\beta^{-/-}$ recipients (Figure 6A). In this setting, only the mature CD4 cells can turn on tdTomato expression and mark the Ebi3 gene transcription. After 15 days of transferring, we detected a clear population that was labeled by tdTomato (Figure 6A). Interestingly, only a fraction of tdTomato⁺ cells (about 20%-50%) kept Thy1.1 (Ebi3) expression in donor CD4⁺ Foxp3⁺ cells (Figure 6A). Subsequently, we determined the phenotype of stable Thy1.1⁺ tdTomato⁺ Tregs and those unstable Thy1.1⁻ tdTomato⁺ Tregs in the transfer model. Of note, stable Thy1.1⁺ tdTomato⁺ Treg cells express much higher ICOS and CD44 but lower CD62L than unstable Thy1.1⁻tdTomato⁺ Tregs (Figure 6B), indicating Thy1.1⁻tdTomato⁺ Tregs could be differentiating intermediates between resting Tregs and stable IL-35-Tregs. Importantly, although Ebi3 genetic traced cells have shown flexibility, tdTomato⁺ labeled cells and IL-10-producing cells fell into two distinct subpopulations (Figure 6C), against the notion that IL-35-Tregs were a general activation stage of effector Treg differentiation. A similar experiment was performed by transferring tdTomato⁻ bone marrow cells into the irradiated host. Clearly, Ebi3 experienced cells have a limited developmental relationship with IL-10-Tregs (Figures 6D and 6E). Together, these genetic tracing data support a notion that IL-35-producing and IL-10-producing Tregs are representative of two unique subsets of eTregs.

Ebi3-Tregs and Blimp1-Tregs Cooperate to Maintain Immune Tolerance

Given the fact that IL-35 and IL-10 were produced by two distinct effector Treg subsets, we asked whether these two subsets have complementary functions *in vivo*. Therefore, we generated 35EbiT × Foxp3GFP-Cre-R26YFP × Blimp1^{flox/flox} transgenic

mice that lack IL-10 expression in Treg cells and could be further ablated for Ebi3⁺ (IL-35) cells by injection of Thy1.1 antibody (Figure 7A). Anti-Thy1.1 antibody was injected into the 35EbiT × Foxp3GFP-Cre-R26YFP × Blimp1^{flox/flox} mice and control groups, and after 15 days, mice were euthanized and analyzed for potential autoimmune phenotypes. In comparison to wild-type mice, singly removing IL-35-producing cells with the anti-Thy1.1 antibody, blocking IL-10 production by conditional knockout of Blimp1 in Tregs, or ablation of both did not decrease the Treg percentage among CD4 T cells. In fact, there was a slight increase in Tregs in the Blimp1 CKO and 35EbiT × Blimp1 CKO groups. However, we found that mice lacking Blimp1 expression in Treg cells alone displayed slightly elevated interferon- γ (IFN- γ ⁺) and IL-17A⁺ CD4⁺ T cells, whereas simultaneous depletion of Ebi3⁺ Treg cells by administration of the anti-Thy1.1 antibody resulted in a synergistic enhancement of both IFN- γ ⁺ and IL-17A⁺ CD4⁺ Tconv cells in spleens (Figure 7A). More importantly, those mice spontaneously develop colitis with a shorter colon length (Figure 7B), accompanied by typical mucosal inflammatory reactions (Figure 7C). These results provide functional evidence, supporting that the two subsets of Treg cells do not play overlapping roles in preventing autoimmune diseases but instead cooperatively contribute to the maintenance of immune homeostasis.

DISCUSSION

Tregs can maintain immune tolerance through multiple suppressive mechanisms. Although these specific mechanisms have been well defined, it is uncertain how Tregs exactly employ these mechanisms and if a single effector Treg utilizes all of those suppressive mechanisms or multiple distinct Treg effectors cooperate together. Producing suppressive cytokines is a key molecular mechanism for Tregs to conduct long-range suppressive functions. In this study, we demonstrated effector Tregs can be divided into two functionally distinct subsets based on their suppressive cytokine induction: IL-35-Tregs are IL-35 producers and express CCR7, preferentially localizing in the T cell zone; and IL-10-Tregs express high levels of IL-10, ICOS, granzymes, and multiple chemokine receptors responsible for migrating to peripheral non-lymphoid tissues. The IL-35-Tregs were distinguished from IL-10-Tregs, not only by their distinct expression signatures, but also in their developmental dependency on a distinct transcriptional factor. Furthermore, we

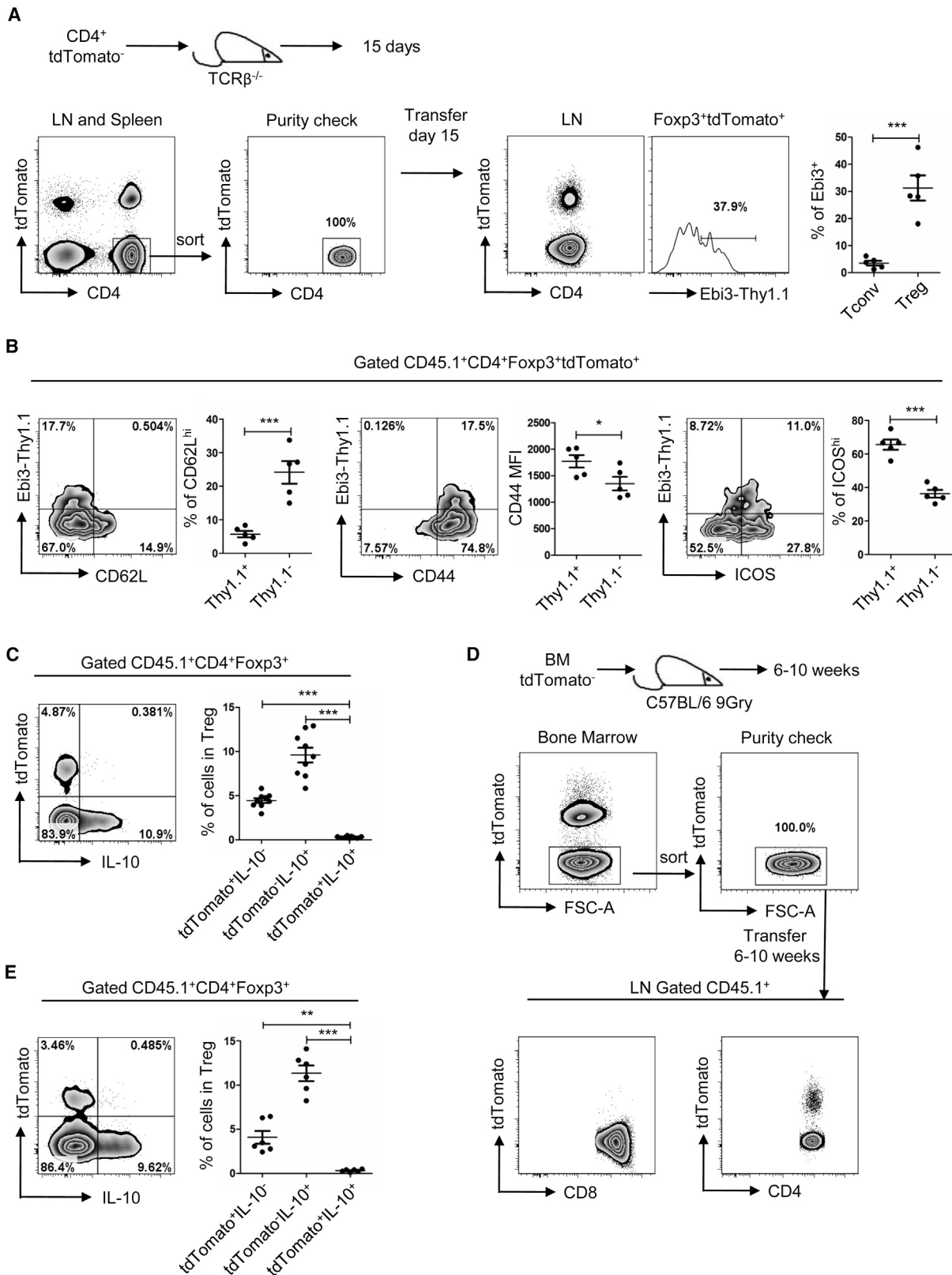
Figure 5. Ebi3-Treg and Blimp1-Treg Have Different Activation Stages and Geographic Locations

(A) Flow cytometric confirmation of the expression of selected genes whose mRNA levels differed between Ebi3-Treg cells and Blimp1-Treg cells as shown in Figure 4. Histogram plot shown are gated on Thy1.1⁻Blimp1⁻ (gray line), Thy1.1⁻Blimp1⁺ (blue line), and Thy1.1⁺Blimp1⁻ (red line) cells (left). The percentages and MFI of the indicated markers are shown (right).

(B) Differential expression genes was confirmed by quantification of PCR in Ebi3-Treg (CD4⁺CD25⁺Thy1.1⁺Blimp1⁻) and Blimp1-Treg (CD4⁺CD25⁺Thy1.1⁻Blimp1⁺) fractions from 35EbiT × Blimp1-GFP KI reporter mice.

(C) For *in vivo* CD4 labeling, anti-CD4 biotin antibody (RM4-4 clone) was intravenously injected, and spleens were harvested 5 min after injection. Splenocytes were examined by flow cytometry after staining with anti-CD4 antibody (RM4-5 clone) and CD25, CD62L, and Thy1.1 (Ebi3). A representative flow cytometry plot depicts the dual-labeled RP/MZ and single-labeled WP CD4⁺CD25⁺CD62L^{low} eTregs. Plots are gated on CD4⁺CD25⁺CD62L^{low} eTregs with secondary gating on specific subsets based on Thy1.1 (Ebi3) and GFP (Blimp1) expression. The histograms (middle panel) and graph (right) show the frequencies of eTregs (Thy1.1⁻Blimp1⁻), Ebi3-Tregs (Thy1.1⁺Blimp1⁻), and Blimp1-Tregs (Thy1.1⁻Blimp1⁺) labeled *in vivo* with CD4-biotin.

The data shown are the typical results from >3 similar experiments (A and C), n ≥ 4; two similar experiments (B), n = 3. Each symbol represents an individual mouse. Error bars represent the mean ± SEM; ns, not significant; *p < 0.05; **p < 0.01; and ***p < 0.001 (ANOVA with Bonferroni post-test [A and C] or Student's t test [B]).



(legend on next page)

provide evidence of Treg activation status controlling the generation of distinct effector Treg subsets that are required for maintenance of immune self-tolerance.

The existence of distinctive subsets of effector Tregs may correspond to control of different types and/or stages of immune responses. Unlike IL-10, which can target multiple cell types, including DCs, macrophages, and T cells (Sabat et al., 2010), IL-35 is more specific to the T cell response. IL-35 binds to an unusual heterodimeric receptor that contains the ubiquitously expressed gp130 as well as IL-12R β 2, which displays restricted expression (Collison et al., 2012). IL-12R β 2 is highly expressed by activated T cells and NKs. Thus, the T cell zone location of IL-35-Tregs would allow them to target auto-reactive T cells more efficiently. In contrast, IL-10-Tregs may have a different responsibility for both controlling the autoimmunity of T cells and suppressing inflammation. Thus, the multi-functional cytokine IL-10 would better fulfill the duty. In addition to IL-10 production, IL-10-Tregs also expressed a high level of GzmB, GzmK, Fgl2, Mmp9, Lgals1, and Lagl3, which could assemble as a distinct Treg effector mechanism for controlling inflammation in local tissue. Thus, the two types of effectors did not play an overlapping role in controlling autoimmunity. The large majority of Tregs in the peripheral organs are generated in the thymus (Klein et al., 2014). During positive and negative selection in the thymus, T cell clones failing to bind self MHC or being too strongly auto-reactive are deleted. Among the surviving T clones, those retaining relatively strong affinity to self-antigens are thought to develop into Tregs, which can recognize both tissue-specific and non-specific antigens (Jordan et al., 2001). Aside from the characteristic of self-antigens themselves, recent studies highlight that the dose of autoreactive thymic antigens has a great impact on the outcome of thymic selection (Malhotra et al., 2016). Because tissue-non-specific antigens are much more abundant than tissue-specific antigens, we speculated that Tregs that recognized tissue-non-specific antigens would have much weaker affinity than that of tissue-specific antigens to avoid death from negative selection. After tTregs mature and migrate to the periphery, different responses can be triggered by different types of self-antigens. Given the fact that IL-35- and IL-10-producing Tregs have a different activation status, it is tempting to speculate that tissue-non-specific Tregs may have a preference to generate central and IL-35-producing cells due to their rather weak affinity. These IL-35-producing cells could generate an

IL-35 suppressive cytokine niche that bystander suppress early T cell priming. In contrast, Tregs recognizing tissue-specific antigens and foreign antigens could have different TCR reactivity, ranging from low to high, due to a lack of efficient negative selection in the thymus. Stronger TCR reactivity could develop into IL-10-producing effector Tregs and gain the capability of migration to conduct suppression of local autoimmune reactions. This model has been supported by the result that anti-CD3 treatment preferentially increases IL-10-Tregs, which could also explain why depleting IL-35-Tregs can boost anti-tumor immune response, whereas treatment with Thy1.1 antibody in Blimp1CKO causes the spontaneously colitis phenotype.

In conclusion, we demonstrated that, based on IL-10 and IL-35 production, Tregs can be diversified into two functionally distinct subsets. Our observations also provide evidence of TCR signal strength tuning the expression of IL-35 and IL-10 during effector Treg differentiation, which represents a mechanism of differential cytokine expression that allows for the tailoring of Treg functional properties to a variety of immune responses. These findings might have an important implication for future clinic therapy.

EXPERIMENTAL PROCEDURES

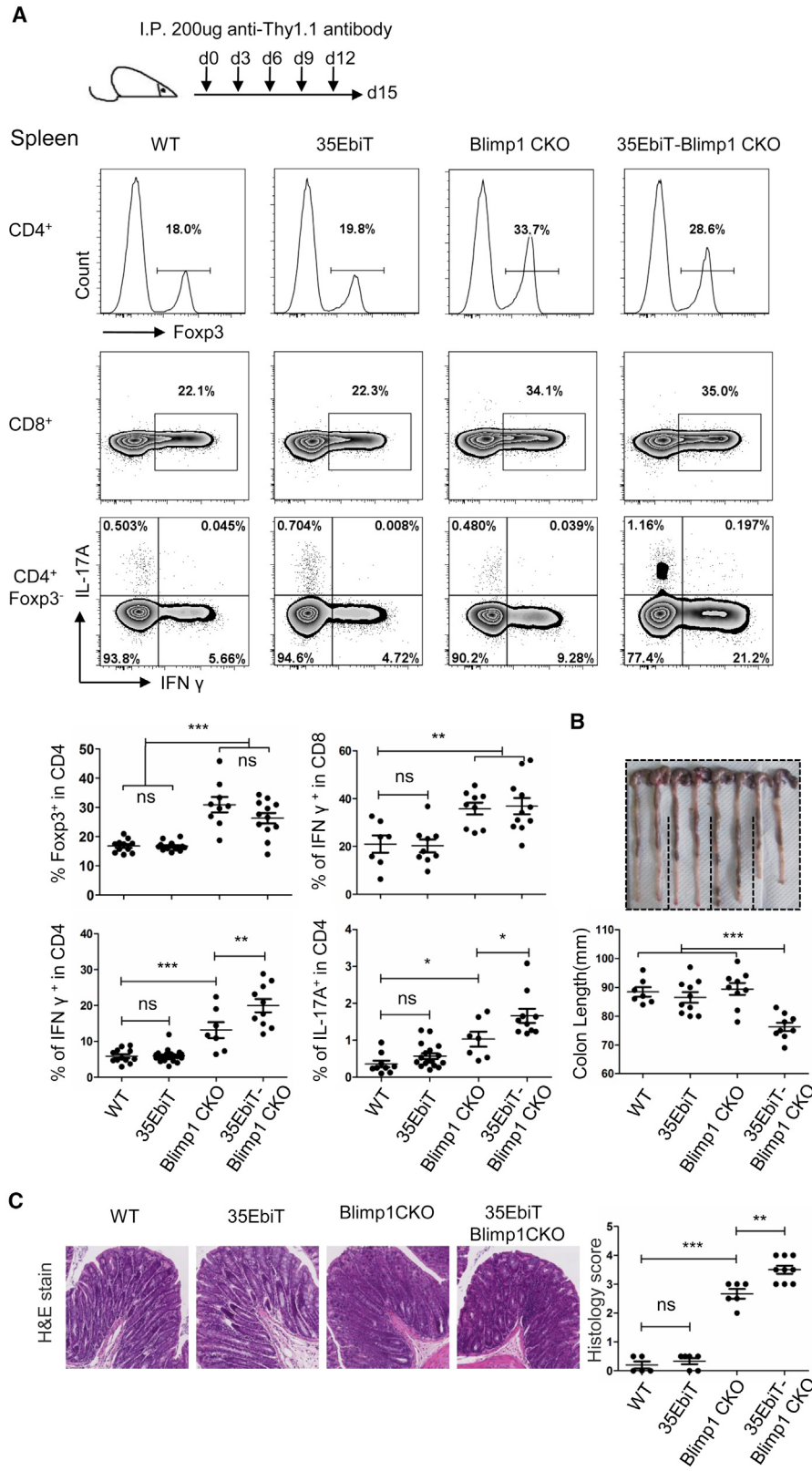
Mice

The Dre-2A-Thy1.1 fusion DNA fragment was inserted by homologous recombination into the ATG translational starting site of a BAC clone (RP23-264G1) bearing the whole Ebi3 locus. The modified BAC was microinjected into the pronuclei of C57BL/6 (B6) fertilized oocytes to generate Ebi3-Dre-2A-Thy1.1 BAC transgenic mice. Mice carrying the reporter cassette Dre-2A-Thy1.1 transgene were screened by fluorescence-activated cell sorting (FACS) analysis or PCR using the mice tail genome. C57BL/6 (B6), CD45.1 $^+$ B6 congenic mice were purchased from the Peking University laboratory animal center (Beijing, China). Foxp3GFP-Cre, R2GFP, and Rosa26-Rox-tdTomato reporter mice have been described (Zhou et al., 2009; Zhang et al., 2017). The Blimp1 $^{fl/fl}$ mice were purchased from Jackson Laboratory (Stock No: 008100). Foxp3-GFP KI mice were gifts from F. Zhang (Institute of Microbiology, Chinese Academy of Sciences [CAS]). Blimp1-GFP KI mice were provided by B. Hou (Institute of Biophysics, CAS) (Kallies et al., 2004). The Foxp3 knockout mice were generated by using CRISPR-Cas9 technology. We designed the single guide RNA (sgRNA) for the targeted exon 2 of the Foxp3 gene, and the sgRNA sequence is 5'-AGGTCCCTCACCCACC TAC-3'. The sgRNA target sequence was cloned into the pX330 (Addgene # 42230) vector, and then the recombinant vector was microinjected into fertilized eggs of B6D2F1 \times B6 at a concentration of 5 ng/ μ L. Founders were genotyped by PCR amplification, followed by DNA sequencing. Foxp3 knockout

Figure 6. IL-35-Tregs Share Limit Developmental Relationship with IL-10-Tregs

- (A) FACS-purified CD45.1 $^+$ CD4 $^+$ tdTomato $^-$ fractions from 35EbiT \times Rosa26-rox-tdTomato reporter mice were intravenously injected into sex-matched TCR β KO recipients at 2×10^6 cells/mouse. Plots were gated on donor CD4 $^+$ T cells, with secondary gating on specific subsets based on Foxp3 and tdTomato expression, and then Thy1.1 (Ebi3) reporter expression was analyzed.
- (B) Plots represent the expression of Thy1.1 and activation makers CD44, CD62L, and ICOS by donor CD4 $^+$ Foxp3 $^+$ tdTomato $^+$ Treg cells at 15 days after transfer.
- (C) Flow cytometry of donor CD4 $^+$ T cells from recipient mice in (A). Plots were gated on CD45.1 $^+$ CD4 $^+$ Foxp3 $^+$ cells. The expression of tdTomato reporter and intracellular IL-10 was analyzed. Average frequencies of tdTomato $^+$ IL-10 $^-$, tdTomato $^-$ IL-10 $^+$, and tdTomato $^+$ IL-10 $^+$ cells among the donor Treg subset are shown.
- (D) FACS purified tdTomato $^-$ bone-marrow cells from 35EbiT \times Rosa26-rox-tdTomato reporter mice were intravenously injected into lethally irradiated C57BL/6 CD45.2 $^+$ recipients at 1×10^7 cells/mouse. Plots were gated on donor CD4 $^+$ and CD8 $^+$ T cells and then tdTomato reporter expression was analyzed.
- (E) Flow cytometry of donor CD4 $^+$ T cells from bone-marrow transplant mice in (D). Plots were gated on CD45.1 $^+$ CD4 $^+$ Foxp3 $^+$ cells. The expression of tdTomato reporter and intracellular IL-10 was analyzed. Average frequencies of tdTomato $^+$ IL-10 $^-$, tdTomato $^-$ IL-10 $^+$, and tdTomato $^+$ IL-10 $^+$ cells among the donor Treg subset are shown.

The data shown are the typical results from 3 similar experiments; $n \geq 5$. Each symbol represents an individual mouse. Error bars represent the mean \pm SEM. * $p < 0.05$, ** $p < 0.01$, and *** $p < 0.001$ (ANOVA with Bonferroni post-test [C and E] or Student's t test [A and B]). See also Figure S6.



(legend on next page)

mice did not express Foxp3 protein and Foxp3^{KO/Y} mice have the same lethal autoimmune phenotype as *Scurfy* mice. All mice were housed in a specific pathogen-free animal facility at the Institute of Microbiology, CAS, in accordance with the guidelines for the care and use of laboratory animals established by the Beijing Association for Laboratory Animal Science. All mouse experiments were performed in accordance with the “Regulation of the Institute of Microbiology, CAS of Research Ethics Committee.” The protocol was approved by the Research Ethics Committee of the Institute of Microbiology, CAS (permit number PZIMCAS2011005).

Antibodies

Labeled anti-Thy1.1 (OX-7), anti-CD25 (PC61), anti-CD44 (IM7), anti-CD69 (H1.2F3), anti-CD38 (90), anti-CD152 (UC10-4B9), anti-CD357 (DTA-1), anti-B220 (RA3-6B2), anti-Helios (22F6), anti-CD5 (53-7.3), anti-IL-10 (JES5-16E3), anti-CD278 (17G9), anti-CD279 (RMP1-30), anti-CD103 (2E7), anti-CD62L (MEL14), anti-CCR7 (4B12), anti-Ly-6a/E(D7), anti-Foxp3 (FJK-16 s), anti-IFN- γ (XMG1.2), anti-IL-17A (eBio17B7), anti-CD4 biotin (RM4-4), anti-CD4 (RM4-5), anti-CD45.1 (A20), anti-CD45.2 (104), and anti-Bcl-2 (BCL/10C4) Fixable Viability Dye eFluor506 were purchased from BD Pharmingen, BioLegend, or eBioscience. Labeled anti-CD4 (GK1.5), anti-CD8 (53-6.7), anti-NK1.1 (PK136), and CD16/32(2.4G2) were purchased from Tianjin Sungene Biotech. Biotinylated Neuropilin-1 PAb (BAF566) was purchased from R&D Systems.

Cell Isolation and Flow Cytometry

Spleens and lymph nodes were collected from the various strains of mice, and single-cell suspensions were prepared by mechanical disruption in DMEM medium supplemented with 2% (v/v) fetal calf serum (FCS). Stained single-cell suspensions were analyzed with an LSRII flow cytometer running FACS Diva (BD Biosciences), and FSC 3.0 files were analyzed and presented with FlowJo Software (Tree Star).

Cytokine Analysis

For cytokine analyses, cells were incubated for 2 to 3 hr at 37°C and 5% CO₂ with 0.5 mM ionomycin, 10 ng/mL PMA, and 3 mM monensin. After surface staining, cells were fixed and made permeable (Foxp3 Staining kit; eBioscience) and were stained for intracellular proteins. For staining Foxp3 with GFP, YFP, and tdTomato, cells were pre-fixed in 1% PFA for 4 min at room temperature, then fixed and permeabilized using the Foxp3 Fixation/Permeabilization kit (eBioscience) and stained with fluorescein-conjugated anti-Foxp3.

Real-Time PCR

Cells isolated from the lymph nodes were purified by flow cytometry, and then RNA was extracted with Trizol. The cDNA was synthesized from total RNA with oligo dT and SuperScript III reverse transcript (Invitrogen). The resultant cDNA served as a template for the amplification of the genes of interest and a house-keeping gene (GAPDH or 18S rRNA) by real-time PCR with the Lightcycler480 Probe Master Mix kit (Roche 04707494001) on a LightCycler480 System (Roche Applied Science). Data are presented and normalized to GAPDH using the comparative Ct method ($\Delta\Delta Ct$), or the mRNA levels of different genes were analyzed by normalization against levels of 18S rRNA. The primers (and probes) used were: 5'-GCTCCCCTGGTTACACTGAA-3' and 5'-ACGGGA TACCGAGAACAT-3' for Ebi3 (probe #26), 5'-TCAGAACATCACAAACCATCA GCA-3' and 5'-CGCCATTATGATTCAAGAGACTG-3' for P35 (probe #49).

Figure 7. Ebi3-Tregs and Blimp1-Tregs Cooperate to Maintain Immune Tolerance

(A) Wild-type, 35EbiT, Blimp1 CKO (Foxp3GFP-Cre-R26YFP × Blimp1^{flox/flox}), and 35EbiT × Blimp1 CKO (35EbiT × Foxp3GFP-Cre-R26YFP × Blimp1^{flox/flox}) mice were administered anti-Thy1.1 antibody (200 µg/time i.p.) five times, with an interval of 2 days, and sacrificed 2 days after the final injection (up). Histogram plots represent the expression of Foxp3 by spleen CD4⁺ T cells after anti-Thy1.1 antibody treatment. Dot plots represent the expression of IFN- γ by spleen CD8⁺ cells and the expression of IFN- γ and IL-17A by spleen CD4⁺Foxp3⁻ cells after the final treatment. Numbers in the plots indicate the percentage of cells in each quadrant (middle). Average frequency of Foxp3⁺/CD4⁺, IFN- γ ⁺/CD8⁺, IFN- γ ⁺/CD4⁺, and IL-17A⁺/CD4⁺ cells among gated subsets are shown (below). (B) Quantification of colon length at the endpoint of the experiment. (C) Histological appearance of the colon at the endpoint of the experiment in mice with colitis compared to healthy mice. Histology score is shown on the right. The data shown are typical results from three experiments, n ≥ 7. Each symbol represents an individual mouse. Error bars represent mean ± SEM; ns, not significant; *p < 0.05; **p < 0.01; and ***p < 0.001 (ANOVA with Bonferroni post-test).

5'-CATGGCATCACCTCTTGAC-3' and 5'-AAGGGCCGAAGTGTGGTA-3' for P28 (probe #38), 5'-TGCAGAGAGGCTCCACTA-3' and 5'-TGGGTTGCTTCCGTTG-3' for Blimp1 (probe #80), 5'-CAGAGCCACATGCTCCTAGA-3' and 5'-TGTCCAGCTGGCTTGTG-3' for IL-10 (probe #41), 5'-CCTAGT GCTGCATGAGGAGA-3' and 5'-TCCACAGACACCACATCAATT-3' for Myc (probe #77), 5'-ACATGCCCTACTTCGATCA-3' and 5'-GCCCCCAAAGTGA CATTATT-3' for GzmB (probe #66), 5'-GGTAAAGGATTCTGCAA-3' and 5'-CCTGAGAGACTAGGGCATGG-3' for GzmK (probe #49), 5'-AGCTGT CATCAACGGGAAG-3' and 5'-TTTGATGTTAGTGGGTCTCG-3' for GAPDH (probe #9), and 5'-GCAATTATCCCCATGAACG-3' and 5'-GGGACTTAAT CAACGCAAGC-3' for 18S rRNA (probe #48).

In Vitro Suppression Assays

Treg suppression assays were performed as described previously, with some modifications (Collison and Vignali, 2011). Single-cell suspensions were prepared from peripheral lymph nodes of 8- to 10-week-old wild-type congenic CD45.1 (BoyJ) mice as responders. Cells were preincubated for 10 min in 5 µM eFluor670 cell proliferation dye (eBioscience) in PBS before culture for proliferation dye dilution analysis. *In vitro* Treg function was measured by culturing 1 × 10⁵ T responders with 1.5 µg/mL soluble anti-CD3 (145-2C11), and titrations of Tregs in complete RPMI (RPMI 1640, 10% FCS, 2 mmol/L L-glutamine, and penicillin/streptomycin). Cells were cultured in a 96-well u-bottom plate at 37°C, 5% CO₂, for 72 hr. Finally, cells were stained with anti-CD45.1, anti-CD4, anti-CD8, and eFluor506 (eBioscience), followed by analysis using an LSRII (BD Biosciences).

Antibody Treatment

Littermate mice were given 200 µg anti-Thy1.1 antibodies (19E14; from Bio X Cell) or 2 µg anti-CD3 antibodies (2C11; from Bio X Cell) by intraperitoneal injection on days 0, 3, 6, 9, and 12 and then sacrificed on day 15 (Thy1.1) or day 12.5 (CD3).

In Vivo T Cell Labeling

Anti-CD4 biotin (2 µg; RM4-4; eBioscience) was injected intravenously and mice were sacrificed 5 min after RM4-4 injection. The spleen was collected and single-cell suspensions were prepared for flow cytometry analysis as described above, with CD4 surface staining using RM4-5 antibodies.

RNA Sequencing

Lymphocytes were isolated from the LN of 35EbiT-Blimp1-GFP KI mice and enriched for CD4⁺ T cells using magnetic beads. Then, CD25⁺CD62L^{low}Thy1.1⁺Blimp1⁻ and CD25⁺CD62L^{low}Thy1.1⁺Blimp1⁺ Tregs were sorted to a typical purity of >90% using Thy1.1, CD25, CD62L, and CD4 Abs. RNA sequencing (RNA-seq) and bioinformatics analysis were conducted by Novogene as described previously (Zhang et al., 2017). Differential expression analysis of two conditions was performed using the DESeq R package (1.20.0). The p values were adjusted using the Benjamini-Hochberg method. Corrected q value = 0.05 and log₂ (fold change) = 1 were set as the threshold for significantly differential expression.

Bone Marrow Transplant

Bone marrow tdTomato⁺ cells sorted from 8- to 10-week-old reporter mice and the resultant bone marrow cells (about 1 × 10⁷ cells) were transferred intravenously into lethally irradiated C57BL/6 CD45.2⁺ recipient mice. Bone-marrow transferred mice were analyzed 6–10 weeks after reconstitution.

Histology Scoring

The colon sections were mildly washed with normal saline, and fecal remnants were removed. Macroscopic inflammation scoring was performed according to the clinical appearance of the colon using the Wallace score. This score rates macroscopic colon lesions on a scale from 0 to 10 based on criteria reflecting inflammation, such as hyperemia, thickening of the bowel, and the extent of ulceration.

Statistical Analysis

FACS data were collected and processed using FACS analysis software (FlowJo). Differences between two datasets were analyzed by ANOVA with Bonferroni post-test or an unpaired two-tailed Student's *t* test with Prism (GraphPad) software. *p* values of less than 0.05 were considered significant. Error bars denote mean \pm SEM.

DATA AND SOFTWARE AVAILABILITY

The accession number for the RNA-seq data reported in this paper is GEO: GSE103456.

SUPPLEMENTAL INFORMATION

Supplemental Information consists of six figures and one table and can be found with this article online at <https://doi.org/10.1016/j.celrep.2017.10.090>.

AUTHOR CONTRIBUTIONS

X.Z. conceived and supervised the project. X.W. modified the BAC constructs for microinjection. J.G. designed the Foxp3 sgRNA, and W.Z. performed the microinjection. X.W. and J.Z. performed the experiments and acquired the data. M.H. and Q.G. performed the experiments. X.W., J.Z., and X.Z. analyzed the data. X.W., J.Z., M.H., and X.Z. wrote the manuscript.

ACKNOWLEDGMENTS

We thank Dr. Alfred Singer, Dr. Vanja Lazarevic, and Dr. Xuguang Tai for critical review of the manuscript and the members of the Alfred Singer laboratory for discussions. We thank Dr. Jitao Guo for assistance in the experiment and thoughtful discussion. We also thank Dr. Baidong Hou and Dr. Mingzhao Zhu for kindly providing of the Blimp1-GFP knockin mice and B16 melanoma cell line, and Dr. Fuping Zhang for providing of the Foxp3-GFP knockin mice. We also gratefully acknowledge Prof. A. Francis Stewart for providing plasmid pCAGGS-Dre-IRES-puro. This work was supported by the NSFC (Grant No. 31670923) and the 973 Program of China (No. 2012CB917102). The authors declare no competing financial interests.

Received: May 27, 2017

Revised: October 9, 2017

Accepted: October 25, 2017

Published: November 14, 2017

REFERENCES

- Abbas, A.K., Benoist, C., Bluestone, J.A., Campbell, D.J., Ghosh, S., Hori, S., Jiang, S., Kuchroo, V.K., Mathis, D., Roncarolo, M.G., et al. (2013). Regulatory T cells: recommendations to simplify the nomenclature. *Nat. Immunol.* **14**, 307–308.
- Bettini, M., and Vignali, D.A. (2009). Regulatory T cells and inhibitory cytokines in autoimmunity. *Curr. Opin. Immunol.* **21**, 612–618.
- Bettini, M., Castellaw, A.H., Lennon, G.P., Burton, A.R., and Vignali, D.A. (2012). Prevention of autoimmune diabetes by ectopic pancreatic β -cell expression of interleukin-35. *Diabetes* **61**, 1519–1526.
- Campbell, D.J. (2015). Control of regulatory T cell migration, function, and homeostasis. *J. Immunol.* **195**, 2507–2513.
- Collison, L.W., and Vignali, D.A. (2011). In vitro Treg suppression assays. *Methods Mol. Biol.* **707**, 21–37.
- Collison, L.W., Workman, C.J., Kuo, T.T., Boyd, K., Wang, Y., Vignali, K.M., Cross, R., Sehy, D., Blumberg, R.S., and Vignali, D.A.A. (2007). The inhibitory cytokine IL-35 contributes to regulatory T-cell function. *Nature* **450**, 566–569.
- Collison, L.W., Chaturvedi, V., Henderson, A.L., Giacomin, P.R., Guy, C., Bankoti, J., Finkelstein, D., Forbes, K., Workman, C.J., Brown, S.A., et al. (2010). IL-35-mediated induction of a potent regulatory T cell population. *Nat. Immunol.* **11**, 1093–1101.
- Collison, L.W., Delgoffe, G.M., Guy, C.S., Vignali, K.M., Chaturvedi, V., Fairweather, D., Satoskar, A.R., Garcia, K.C., Hunter, C.A., Drake, C.G., et al. (2012). The composition and signaling of the IL-35 receptor are unconventional. *Nat. Immunol.* **13**, 290–299.
- Cretney, E., Xin, A., Shi, W., Minnich, M., Masson, F., Miasari, M., Belz, G.T., Smyth, G.K., Busslinger, M., Nutt, S.L., et al. (2011). The transcription factors Blimp-1 and IRF4 jointly control the differentiation and function of effector regulatory T cells. *Nat. Immunol.* **12**, 304–311.
- Cretney, E., Kallies, A., and Nutt, S.L. (2013). Differentiation and function of Foxp3(+) effector regulatory T cells. *Trends Immunol.* **34**, 74–80.
- Ding, Y., Xu, J., and Bromberg, J.S. (2012). Regulatory T cell migration during an immune response. *Trends Immunol.* **33**, 174–180.
- Gondek, D.C., Lu, L.F., Quezada, S.A., Sakaguchi, S., and Noelle, R.J. (2005). Cutting edge: contact-mediated suppression by CD4+CD25+ regulatory cells involves a granzyme B-dependent, perforin-independent mechanism. *J. Immunol.* **174**, 1783–1786.
- Hori, S. (2014). Lineage stability and phenotypic plasticity of Foxp3⁺ regulatory T cells. *Immunol. Rev.* **259**, 159–172.
- Huang, C.H., Loo, E.X.L., Kuo, I.C., Soh, G.H., Goh, D.L.M., Lee, B.W., and Chua, K.Y. (2011). Airway inflammation and IgE production induced by dust mite allergen-specific memory/effector Th2 cell line can be effectively attenuated by IL-35. *J. Immunol.* **187**, 462–471.
- Jordan, M.S., Boesteanu, A., Reed, A.J., Petrone, A.L., Holenbeck, A.E., Lerman, M.A., Naji, A., and Caton, A.J. (2001). Thymic selection of CD4+CD25+ regulatory T cells induced by an agonist self-peptide. *Nat. Immunol.* **2**, 301–306.
- Kallies, A., Hasbold, J., Tarlinton, D.M., Dietrich, W., Corcoran, L.M., Hodgkin, P.D., and Nutt, S.L. (2004). Plasma cell ontogeny defined by quantitative changes in blimp-1 expression. *J. Exp. Med.* **200**, 967–977.
- Kamanaka, M., Kim, S.T., Wan, Y.Y., Sutterwala, F.S., Lara-Tejero, M., Galán, J.E., Harhaj, E., and Flavell, R.A. (2006). Expression of interleukin-10 in intestinal lymphocytes detected by an interleukin-10 reporter knockin tiger mouse. *Immunity* **25**, 941–952.
- Klein, L., Kyewski, B., Allen, P.M., and Hogquist, K.A. (2014). Positive and negative selection of the T cell repertoire: what thymocytes see (and don't see). *Nat. Rev. Immunol.* **14**, 377–391.
- Komatsu, N., and Hori, S. (2007). Full restoration of peripheral Foxp3⁺ regulatory T cell pool by radioresistant host cells in scurfy bone marrow chimeras. *Proc. Natl. Acad. Sci. USA* **104**, 8959–8964.
- Levine, A.G., Arvey, A., Jin, W., and Rudensky, A.Y. (2014). Continuous requirement for the TCR in regulatory T cell function. *Nat. Immunol.* **15**, 1070–1078.
- Li, M.O., and Rudensky, A.Y. (2016). T cell receptor signalling in the control of regulatory T cell differentiation and function. *Nat. Rev. Immunol.* **16**, 220–233.
- Liston, A., and Gray, D.H. (2014). Homeostatic control of regulatory T cell diversity. *Nat. Rev. Immunol.* **14**, 154–165.
- Malhotra, D., Linehan, J.L., Dileepan, T., Lee, Y.J., Purtha, W.E., Lu, J.V., Nelson, R.W., Fife, B.T., Orr, H.T., Anderson, M.S., et al. (2016). Tolerance is established in polyclonal CD4(+) T cells by distinct mechanisms, according to self-peptide expression patterns. *Nat. Immunol.* **17**, 187–195.
- Mari, E.R., Rasouli, J., Cric, B., Moore, J.N., Conejo-Garcia, J.R., Rajasagi, N., Zhang, G.X., Rabinovich, G.A., and Rostami, A. (2016). Galectin-1 is essential for the induction of MOG35–55 -based intravenous tolerance in experimental autoimmune encephalomyelitis. *Eur. J. Immunol.* **46**, 1783–1796.
- Martins, G., and Calame, K. (2008). Regulation and functions of Blimp-1 in T and B lymphocytes. *Annu. Rev. Immunol.* **26**, 133–169.

- Moreira, A.P., Cavassani, K.A., Massafera Tristão, F.S., Campanelli, A.P., Martinez, R., Rossi, M.A., and Silva, J.S. (2008). CCR5-dependent regulatory T cell migration mediates fungal survival and severe immunosuppression. *J. Immunol.* **180**, 3049–3056.
- Ohkura, N., Hamaguchi, M., Morikawa, H., Sugimura, K., Tanaka, A., Ito, Y., Osaki, M., Tanaka, Y., Yamashita, R., Nakano, N., et al. (2012). T cell receptor stimulation-induced epigenetic changes and Foxp3 expression are independent and complementary events required for Treg cell development. *Immunity* **37**, 785–799.
- Pandian, P., and Zhu, J. (2015). Origin and functions of pro-inflammatory cytokine producing Foxp3+ regulatory T cells. *Cytokine* **76**, 13–24.
- Sabat, R., Grütz, G., Warszawska, K., Kirsch, S., Witte, E., Wolk, K., and Geiginat, J. (2010). Biology of interleukin-10. *Cytokine Growth Factor Rev.* **21**, 331–344.
- Sakaguchi, S. (2004). Naturally arising CD4+ regulatory t cells for immunologic self-tolerance and negative control of immune responses. *Annu. Rev. Immunol.* **22**, 531–562.
- Shalev, I., Liu, H., Kosciuk, C., Bartczak, A., Javadi, M., Wong, K.M., Maknojia, A., He, W., Liu, M.F., Diao, J., et al. (2008). Targeted deletion of fgl2 leads to impaired regulatory T cell activity and development of autoimmune glomerulonephritis. *J. Immunol.* **180**, 249–260.
- Smigiel, K.S., Richards, E., Srivastava, S., Thomas, K.R., Dudda, J.C., Klonowski, K.D., and Campbell, D.J. (2014). CCR7 provides localized access to IL-2 and defines homeostatically distinct regulatory T cell subsets. *J. Exp. Med.* **211**, 121–136.
- Stefanová, I., Dorfman, J.R., and Germain, R.N. (2002). Self-recognition promotes the foreign antigen sensitivity of naive T lymphocytes. *Nature* **420**, 429–434.
- Szymczak, A.L., Workman, C.J., Wang, Y., Vignali, K.M., Dilioglou, S., Vanin, E.F., and Vignali, D.A. (2004). Correction of multi-gene deficiency in vivo using a single 'self-cleaving' 2A peptide-based retroviral vector. *Nat. Biotechnol.* **22**, 589–594.
- Turnis, M.E., Sawant, D.V., Szymczak-Workman, A.L., Andrews, L.P., Delgoffe, G.M., Yano, H., Beres, A.J., Vogel, P., Workman, C.J., and Vignali, D.A. (2016). Interleukin-35 limits anti-tumor immunity. *Immunity* **44**, 316–329.
- Vasantha Kumar, A., Moro, K., Xin, A., Liao, Y., Gloury, R., Kawamoto, S., Fagarasan, S., Mielke, L.A., Afshar-Sterle, S., Masters, S.L., et al. (2015). The transcriptional regulators IRF4, BATF and IL-33 orchestrate development and maintenance of adipose tissue-resident regulatory T cells. *Nat. Immunol.* **16**, 276–285.
- Vignali, D.A., Collison, L.W., and Workman, C.J. (2008). How regulatory T cells work. *Nat. Rev. Immunol.* **8**, 523–532.
- Yurchenko, E., Tritt, M., Hay, V., Shevach, E.M., Belkaid, Y., and Piccirillo, C.A. (2006). CCR5-dependent homing of naturally occurring CD4+ regulatory T cells to sites of Leishmania major infection favors pathogen persistence. *J. Exp. Med.* **203**, 2451–2460.
- Zhang, Z., Zhang, W., Guo, J., Gu, Q., Zhu, X., and Zhou, X. (2017). Activation and functional specialization of regulatory T cells lead to the generation of Foxp3 instability. *J. Immunol.* **198**, 2612–2625.
- Zhou, X., Bailey-Bucktrout, S.L., Jeker, L.T., Penaranda, C., Martínez-Llordera, M., Ashby, M., Nakayama, M., Rosenthal, W., and Bluestone, J.A. (2009). Instability of the transcription factor Foxp3 leads to the generation of pathogenic memory T cells in vivo. *Nat. Immunol.* **10**, 1000–1007.